Dalton Transactions

ROYAL SOCIETY OF CHEMISTRY

PAPER

View Article Online
View Journal | View Issue

Cite this: *Dalton Trans.*, 2024, **53**, 16280

Adducts of Lewis acidic stibanes with phosphane chalcogenides†

Jonas Krieft, Hannah Koch, Beate Neumann, Hans-Georg Stammler, Jan-Hendrik Lamm, Andreas Mix and Norbert W. Mitzel *

Received 8th August 2024,
Accepted 11th September 2024

DOI: 10.1039/d4dt02268h

rsc.li/dalton

Starting from $ClSbR^F_2$ (R^F = C_2F_5, 3,5-$(CF_3)_2C_6H_3$) and $H(E)P(tBu)_2$ (E = O, S), we prepared the oxy- and sulphanediyl-bridged adducts $R^F_2Sb(Cl)–E–(H)P(tBu)_2$, which are stable against the elimination of HCl. The different electron-withdrawing substituents and chalcogen bridging units influence the size of the Sb–E–P angle. $ClSb(C_2F_5)_2$ and nBu_3SnH react to give $HSb(C_2F_5)_2$, which seems to interact weakly with $H(O)P(tBu)_2$ in solution as observed *via* NMR. All products were characterised by NMR spectroscopy and all the stable ones were additionally characterised by X-ray diffraction and elemental analyses.

Introduction

The neutralisation reaction of Lewis acids and bases can be suppressed by steric shielding, as observed by Brown *et al.* 82 years ago by contrasting the reaction of 2,6-lutidine with BF_3 and the absence of a reaction with the bulkier $B(CH_3)_3$.[1] These inter- or even intramolecular Lewis acid/base combinations still have untapped reaction potential. The investigation of such "Frustrated Lewis Pairs" (FLP) was decisively initiated and promoted by Stephan and Erker, who presented the first FLP systems by combining boron-containing Lewis acids and phosphorus-based Lewis bases.[2] Within the last two decades, this high level of interest has led to an ever-expanding repertoire of functional building blocks, *e.g.* those based on tetrels,[3–6] rare-earth metals[7] or d-block elements,[8] in addition to the Lewis acid centres of boron and aluminium,[9] which are usually considered to be the most common. A wide range of reactions such as C–H activation, hydrogen and small molecule activation and CO_2 reduction are accessible with these systems.[10,11] The use of strongly electron-withdrawing pentafluoroethyl groups allowed the monitoring of intramolecular FLP systems of type $(F_5C_2)_nECH_2P(tBu)_2$ (E = Si, Ge, Sn with n = 3 and Sb with n = 2) and the observation of the activation of substrates such as CO_2, H_2 and unsaturated systems typical of some of these FLPs.[4–6,12–14] The bis(pentafluoroethyl)stibanyl function, $(F_5C_2)_2Sb–$, with its lone pair at the Sb(III) atom, represents a soft Lewis acid whose reactivity follows Pearson's HSAB concept.[13–15] These results complement the work by Gabbaï *et al.* on antimony-based Lewis acid systems, such as stibonium cations and various stiboranes for the detection and transport of (fluoride) anions.[16]

We have succeeded in chelating various halides and (nitrogen-based) Lewis bases in the form of pnictogen bonding with anthracene-based systems, which bear $–C{\equiv}C–Sb(C_2F_5)_2$ functions.[17,18]

Stephan and Erker provided a proficient insight into the crucial importance of the bridging unit and the orientation of the (interacting) opposing functions in intramolecular FLPs with respect to dihydrogen cleavage or adduct formation.[11] The study of chalcogen-based spacers has so far received less attention. Only a few examples from Stephan,[19] Wang,[20] and our own research group exist in the form of B/Al/Si–O–P FLPs.[21,22]

In this work we aim to combine our established bis(pentafluoroethyl)stibanyl function ($(F_5C_2)_2Sb–$) with the chalcogen spacer motif and investigate the adducts formed.

Results and discussion

Starting from $MesSbCl_2$ (**1**) and following synthesis of $(F_5C_2)_2SbMes$ (**2**, Mes = mesityl, Scheme 1), we have optimised the synthesis of the previously presented antimony reagent $(F_5C_2)_2SbCl$ (**3**),[17] finally avoiding the occurrence of a mixture with the cleavage product from the deprotection of the protected precursors. Unlike toluene, which is formed by cleaving a toluyl protecting group, mesitylene, which is formed by reacting **2** with hydrogen chloride, can be separated by distillation due to its higher boiling point difference from **3**.

The reported synthesis[23] of **1** yielded crystals, suitable for X-ray diffraction experiments. The solid-state structure of **1**

Chair of Inorganic and Structural Chemistry, Center for Molecular Materials CM$_2$, Faculty of Chemistry, Bielefeld University, Universitätsstraße 25, 33615 Bielefeld, Germany. E-mail: mitzel@uni-bielefeld.de

†Electronic supplementary information (ESI) available. CCDC 2367656–2367665. For ESI and crystallographic data in CIF or other electronic format see DOI: https://doi.org/10.1039/d4dt02268h

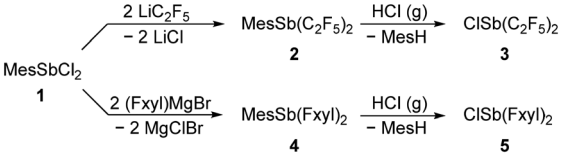

Scheme 1 Synthesis of **3** and **5** from $MesSbCl_2$ (**1**, Mes = mesityl) over the protected precursors **2** and **4**.

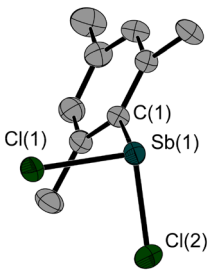

Fig. 1 Molecular structure of **1** in the solid state with three molecules in the asymmetric unit. For clarity, only one molecule is depicted and the hydrogen atoms are omitted. Ellipsoids are set at 50% probability. Selected bond lengths [Å] and angles [°]: Sb(1)–Cl(1) 2.395(1), Sb(1)–Cl(2) 2.381(1), Sb(1)–C(1) 2.150(2), Sb(2)–Cl(3) 2.387(1), Sb(2)–Cl(4) 2.376(1), Sb(2)–C(10) 2.134(3), Sb(3)–Cl(5) 2.381(1), Sb(3)–Cl(6) 2.377(1), Sb(3)–C(19) 2.143(2); Cl(1)–Sb(1)–Cl(2) 92.0(1), Cl(1)–Sb(1)–C(1) 97.5(1), Cl(2)–Sb(1)–C(1) 101.4(1), Cl(3)–Sb(2)–Cl(4) 94.5(1), Cl(3)–Sb(2)–C(10) 101.6(1), Cl(4)–Sb(2)–C(10) 97.0(1), Cl(5)–Sb(3)–Cl(6) 95.3(1), Cl(5)–Sb(3)–C(19) 96.9(1), Cl(6)–Sb(3)–C(19) 100.4(1).

(Fig. 1) with its three molecules in the asymmetric unit shows Sb–Cl bond lengths of 2.376(1)–2.395(1) Å and Sb–C bond lengths of 2.134(3)–2.150(2) Å. The Cl–Sb–Cl angles are smaller (92.0(1)–95.3(1)°) than the Cl–Sb–C angles (96.9(1)–101.6(1)°).

The solid-state structure of liquid **2** (Fig. 2) was determined *via in situ* crystallisation on the diffractometer. The Sb(1)–C(1) bond lengths in **1** and **2** are quite the same. The other two Sb–C bonds in **2** are about 0.1 Å longer than the Sb(1)–C(1) bond.

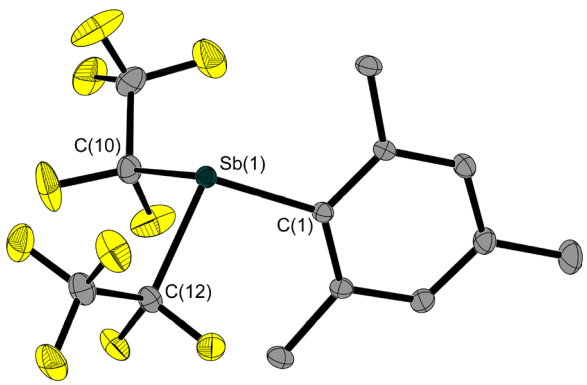

Fig. 2 Molecular structure of **2** in the solid state. Ellipsoids are set at 50% probability. The hydrogen atoms are omitted for clarity. Selected bond lengths [Å] and angles [°]: Sb(1)–C(1) 2.152(1), Sb(1)–C(10) 2.240(1), Sb(1)–C(12) 2.246(1); C(1)–Sb(1)–C(10) 98.3(1), C(1)–Sb(1)–C(12) 103.1(1), C(10)–Sb(1)–C(12) 92.7(1).

The NMR data for **2** and **3** in CD_2Cl_2 show the typical splitting pattern for pentafluoroethylstibanyl functions.[17,18,24] The $^{13}C\{^1H\}$ NMR spectra show triplets of quartets (**2**: 121.8 ppm, **3**: 126.4 ppm, CF_2) and quartets of triplets (**2**: 120.4 ppm, **3**: 120.3 ppm CF_3) and the ^{19}F NMR spectra contain multiplets of the CF_3 unit (**2**: −83.2 ppm, **3**: −81.3 ppm) and broad multiplets of the AB-spin systems of the CF_2 units (**2**: −106.4/−107.2 ppm, **3**: −111.8/−112.3 ppm), respectively.

We have now succeeded in determining the solid-state structure of **3**, which is liquid at room temperature. A single crystal, suitable for X-ray diffraction, was grown on the diffractometer by *in situ* crystallisation. After establishing a solid–liquid equilibrium at 235 K and manually melting all but a tiny seed crystal (using a piece of wire for warming), the sample was cooled to 100 K to achieve its complete crystallization. The molecular structure of **3** (Fig. 3) shows an Sb–Cl bond length of 2.356(1) Å. As is common for trisubstituted pnictogen atoms in the oxidation state +III, the antimony atom is trigonal-pyramidal coordinated with angles involving the Sb atom ranging between 92.8(1)° and 88.5(1)°.

In order to investigate the influence of the electron-withdrawing substituents on the structure of Sb–E–P systems, we also synthesised the mesityl-protected $Fxyl_2SbMes$ (**4**, Fxyl = bis(trifluoromethyl)phenyl) starting from dichloromesitylstibane (**1**, Scheme 1). Subsequent deprotection of compound **4** with hydrogen chloride resulted in $Fxyl_2SbCl$ (**5**, Scheme 1). The aryl-type Fxyl substituent allows the use of less stringent conditions for the cleavage of the mesityl protecting group.

The solid-state structures of **4** (Fig. 4) and **5** (Fig. 5) also show the striking trigonal-pyramidal structural motif around the antimony atom. The Sb–Cl bond in compound **4** is significantly longer (2.504(1) Å) compared to that in **3** (0.15 Å), which is due to the pentafluoroethyl groups in **3**. In general, all Sb–E bonds in **4** and **5** are longer than the corresponding bonds in the pentafluoroethyl analogues **2** and **3**.

The reaction of **3** with di-*tert*-butylphosphane oxide afforded the oxy-bridged compound **6** in almost quantitative yield. In contrast to Wang and Stephan, who observed the formation of the aforementioned oxy bridge and also the elimination of hydrogen chloride in the reaction of chloroboranes with di-mesitylphosphane oxide[19,20] and di-*tert*-butylphosphane oxide,[19] respectively, we observed the formation of the Sb–O bond but did not observe the release of hydrogen chloride (Scheme 2).

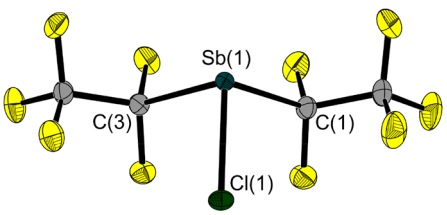

Fig. 3 Molecular structure of **3** in the solid state. Ellipsoids are set at 50% probability. Selected bond lengths [Å] and angles [°]: Sb(1)–Cl(1) 2.356(1), Sb(1)–C(1) 2.252(1), Sb(1)–C(3) 2.243(1); C(1)–Sb(1)–Cl(1) 92.8(1), C(3)–Sb(1)–Cl(1) 91.2(1), C(1)–Sb(1)–C(3) 88.5(1).

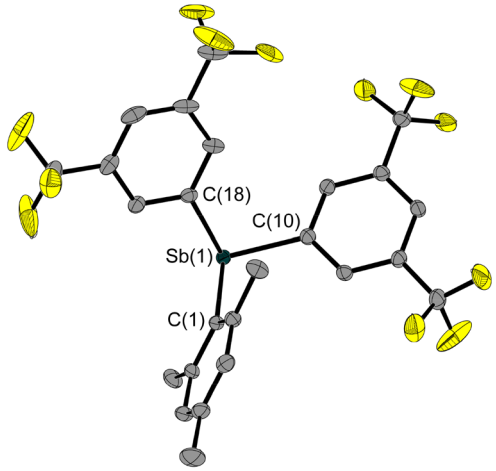

Fig. 4 Molecular structure of **4**. Ellipsoids are set at 50% probability; hydrogen atoms and the disorder of one trifluoromethyl group are omitted for clarity. Selected bond lengths [Å] and angles [°]: Sb(1)–C(1) 2.160(2), Sb(1)–C(10) 2.162(2), Sb(1)–C(18) 2.167(2); C(1)–Sb(1)–C(10) 99.4(1), C(1)–Sb(1)–Cl(18) 96.1(1), C(10)–Sb(1)–C(18) 97.7(1).

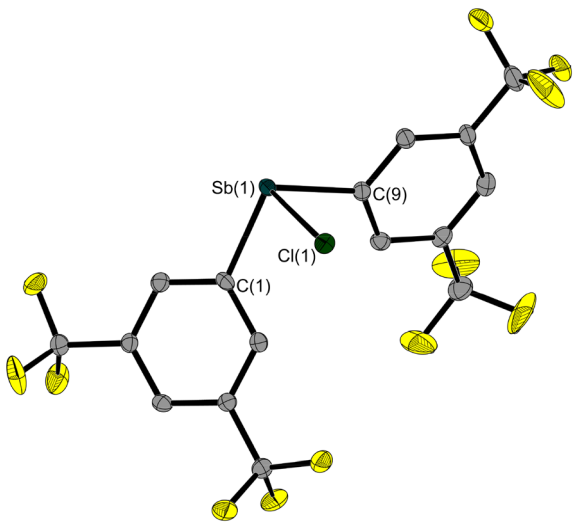

Fig. 5 Molecular structure of **5** in the solid state. Ellipsoids are set at 50% probability; hydrogen atoms and the disorder of one trifluoromethyl group are omitted for clarity. Selected bond lengths [Å] and angles [°]: Sb(1)–Cl(1) 2.504(1), Sb(1)–C(1) 2.151(3), Sb(1)–C(9) 2.152(3); C(1)–Sb(1)–Cl(1) 91.0(1), C(9)–Sb(1)–Cl(1) 87.8(1), C(1)–Sb(1)–C(9) 99.3(1).

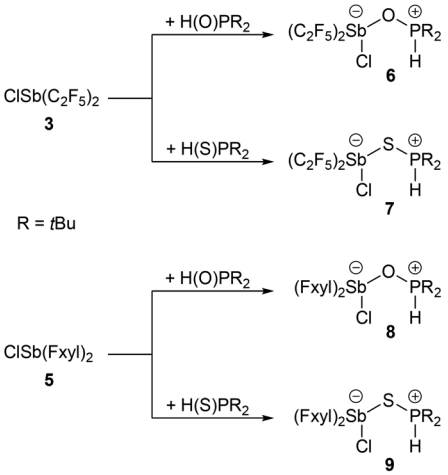

Scheme 2 Synthesis of the pentafluoroethyl-substituted adducts **6** and **7** from **3**, and the Fxyl-substituted adducts **8** and **9** from **5**, with $H(O)PtBu_2$ and $H(S)PtBu_2$, respectively.

Because of the non-spontaneous elimination of HCl, we attempted to abstract the chlorine atom and the hydrogen atom of **6** under more severe conditions by conversion with lithium and potassium hexamethyldisilazide, trityl lithium and *n*-butyl lithium and various amines, respectively; in all cases the corresponding NMR spectra showed only unselective decomposition or, in the case of the amines, no reaction.

In compound **6**, both the chlorine substituent on the pentafluoroethylstibanyl function and the hydrogen atom of the phosphane precursor are still present. The latter can be detected particularly well in the proton NMR spectrum of compound **6**, which contains a doublet with a characteristically large $^1J_{P,H}$ coupling constant of 447 Hz at a chemical shift of 6.03 ppm.

The excellent crystallisation behaviour enabled us to investigate the structure of **6** using X-ray diffraction. Its solid-state structure (Fig. 6) shows the adduct formation *via* the Sb–O bond and a bent Sb–O–P backbone. This has a rather obtuse angle at 147.5(1)°, while the O–Sb–Cl angle is even more obtuse at 167.9(1)°, and therefore close to linearity. The antimony atom is bisphenoidally surrounded by its substituents due to its lone pair.

The distance between the chlorine substituent and the hydrogen atom, whose position has been refined, may be an indication of why intramolecular elimination of hydrogen chloride does not occur spontaneously.

The Sb–O bond length of 2.273(2) Å is within the expected range for Sb–O bonds.[14] The formation of this Sb–O bond slightly lengthens the P–O bond (1.503(2) Å) compared to that of the reactant $H(O)P(tBu)_2$ (1.482(2) Å),[25] while the Sb–Cl bond in **6** (2.470(1) Å) is significantly longer than that in **3** (2.356(1) Å).

We synthesised $H(S)P(tBu)_2$ from hydrogen sulphide and di-*tert*-butylchlorophosphane in the same way as $H(O)P(tBu)_2$.[21] As in **6**, a doublet with a large coupling constant (420 Hz), at 5.77 ppm in the ^{1}H NMR spectrum, is detected for the sulphanediyl-bridged compound **7**.

In the solid-state structure of **7** (Fig. 6), the large difference in conformation compared to compound **6** is immediately apparent; the Sb–S–P backbone has an angle of 98.5(1)°, which is almost 50° smaller. However, the E–Sb–Cl angles in **6** and **7** are quite similar (Table 1). As expected, the bonds involving the larger sulphur atom rather than the oxygen atom are about 0.5 Å longer. The Sb–Cl bond is also more extended compared to that in **3** and **6**. The structure of the central bridging unit

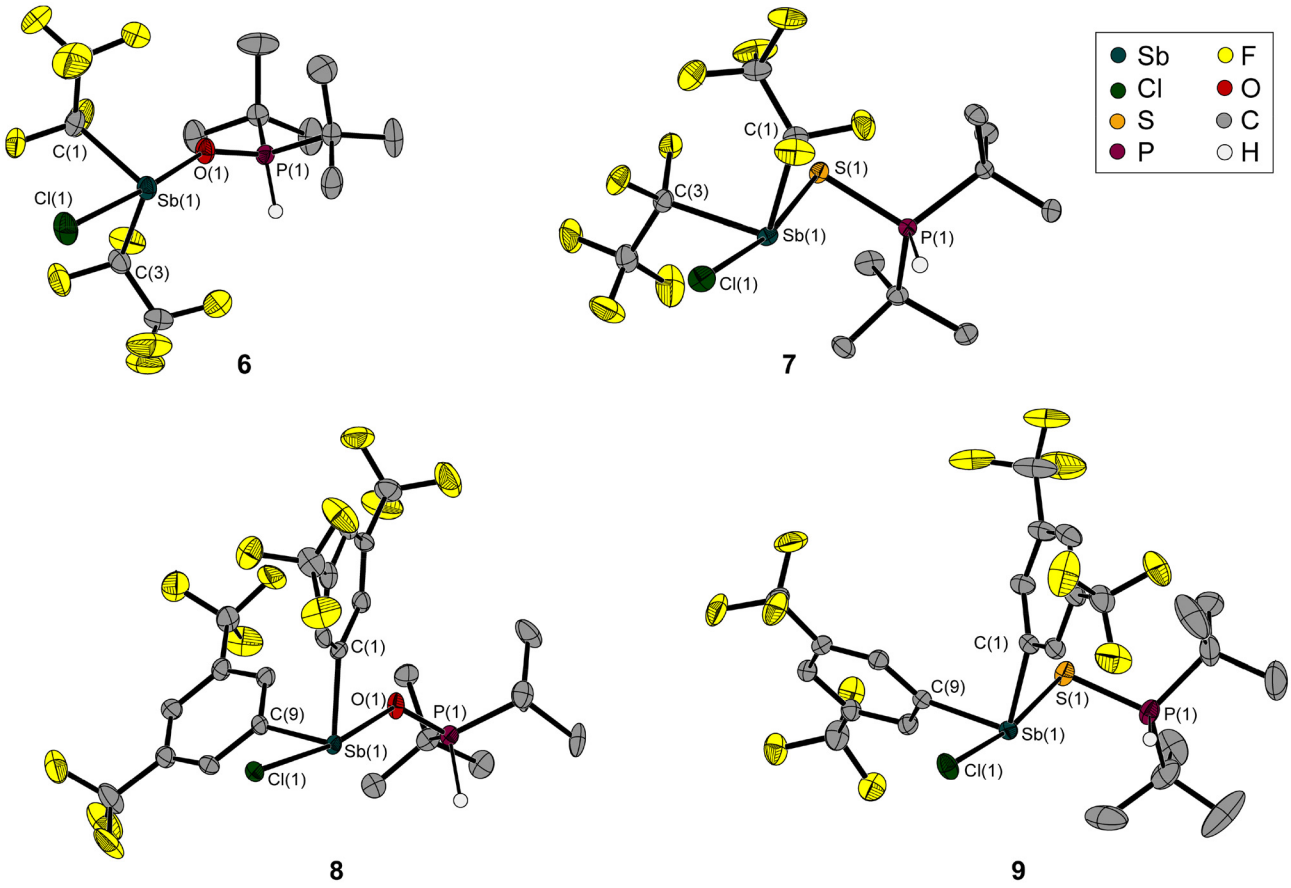

Fig. 6 Molecular structures of **6**, **7**, **8** and **9**. Ellipsoids are set at 50% probability; hydrogen atoms except those of P–**H** and the disordered parts of **6**, **8** and **9** are omitted for clarity. Selected bond lengths [Å] and angles [°]: **6**: Sb(1)–Cl(1) 2.470(1), Sb(1)–O(1) 2.273(2), Sb(1)–C(1) 2.267(3), Sb(1)–C(3) 2.285(4), P(1)–O(1) 1.503(2); O(1)–Sb(1)–Cl(1) 167.9(1), O(1)–Sb(1)–C(1) 81.8(1), O(1)–Sb(1)–C(3) 82.2(1), C(1)–Sb(1)–Cl(1) 89.0(1), C(1)–Sb(1)–C(3) 88.6(1), C(3)–Sb(1)–Cl(1) 89.8(1), Sb(1)–O(1)–P(1) 147.5(1); **7**: Sb(1)–Cl(1) 2.486(1), Sb(1)–S(1) 2.751(1), Sb(1)–C(1) 2.260(1), Sb(1)–C(3) 2.267(1), P(1)–S(1) 2.010(1); Cl(1)–Sb(1)–S(1) 169.1(1), C(1)–Sb(1)–Cl(1) 89.6(1), C(1)–Sb(1)–S(1) 87.9(1), C(1)–Sb(1)–C(3) 98.5(1), C(3)–Sb(1)–Cl(1) 86.8(1), C(3)–Sb(1)–S(1) 83.2(1), Sb(1)–S(1)–P(1) 98.5(1); **8**: Sb(1)–Cl(1) 2.505(2), Sb(1)–O(1) 2.348(5), Sb(1)–C(1) 2.168(9), Sb(1)–C(9) 2.183(9), P(1)–O(1) 1.525(6); Cl(1)–Sb(1)–O(1) 170.4(2), C(1)–Sb(1)–Cl(1) 90.8(2), C(1)–Sb(1)–O(1) 84.0(3), C(1)–Sb(1)–C(9) 95.0(3), C(9)–Sb(1)–Cl(1) 90.1(2), C(9)–Sb(1)–O(1) 82.3(3), Sb(1)–O(1)–P(1) 131.0(4); **9**: Sb(1)–Cl(1) 2.520(1), Sb(1)–S(1) 2.829(1), Sb(1)–C(1) 2.157(2), Sb(1)–C(9) 2.147(2), P(1)–S(1) 1.995(1); Cl(1)–Sb(1)–S(1) 171.4(1), C(1)–Sb(1)–Cl(1) 88.2(1), C(1)–Sb(1)–S(1) 87.0(1), C(1)–Sb(1)–C(9) 97.4(1), C(9)–Sb(1)–Cl(1) 90.4(1), C(9)–Sb(1)–S(1) 83.3(1), Sb(1)–S(1)–P(1) 95.2(1).

Table 1 Selected angles and bond lengths of chlorostibanes **3** and **5** and of their corresponding adducts with phosphane oxides (**6**, **8**) and phosphane sulphides (**7**, **9**). Reactant bond lengths: P–O(H(O)P(*t*Bu)$_2$) 1.482(2) Å,[25] P–S(H(S)P(*t*Bu)$_2$) 1.967(1) Å,[26] Sb–Cl(**3**) 2.356(1) Å, and Sb–Cl(**7**) 2.504(1) Å

	Sb–E–P [°]	Cl–Sb–E [°]	Sb–E [Å]	Sb–Cl [Å]	P–E [Å]
H(O)P(*t*Bu)$_2$	—	—	—	—	1.482(2)[23]
H(S)P(*t*Bu)$_2$	—	—	—	—	1.967(1)[24]
3	—	—	—	2.356(1)	—
6 (E = O)	147.5(1)	167.9(1)	2.273(2)	2.470(1)	1.503(2)
7 (E = S)	98.5(1)	169.1(1)	2.751(1)	2.486(1)	2.010(1)
5	—	—	—	2.504(1)	—
8 (E = O)	131.0(4)	170.4(2)	2.348(5)	2.505(2)	1.525(6)
9 (E = S)	95.2(1)	171.4(1)	2.829(1)	2.520(1)	1.995(1)

thus follows a known behaviour: the central chalcogen-including angle is narrower in sulphanediyl- than in oxy-bridged molecules, as can be seen in the reported gas-phase structures of distibanyl oxide $(Me_2Sb)_2O$ (131.1(2)°)[27]/distibanyl sulfide $(Me_2Sb)_2O$ (104.5(5)°)[28] and disiloxane $(H_3Si)_2O$ (144.1(9)°)[29]/disilthiane $(H_3Si)_2S$ (108.7(3)°).[30] Substitution with electronegative groups leads to an increase in these angles ($H_3SiOSiH_3$: 144.1(9)°,[29] $Cl_3SiOSiCl_3$: 146(4)°,[31] $F_3SiOSiF_3$: 155.7(2)°).[32]

The oxy- and sulphanediyl-bridged adducts **8** and **9** were synthesised from **7** in the same way as compounds **6** and **7** (Scheme 2). As for **6** and **7**, the proton and ^{31}P NMR spectra confirm the presence of the hydrogen atom of the phosphonium function in **8** and **9** (Table 2).

As expected, the molecular structure of **8** (Fig. 6) contains the previously observed bent structural motif with an obtuse Sb–O–P angle, which is 16° narrower than in compound **6**. At the same time, the Cl–Sb–E angle is slightly more compressed at 170.4(2)°. Compared to **6**, all bonds containing oxygen and chlorine are longer.

The molecular structure of **9** (Fig. 6) matches the expectations, based on the structural parameters of **6**, **7** and **8**. The sulphanediyl-bridging unit results in an Sb–S–P angle close to 90°, which is the smallest of all the structures discussed here (Table 1). This is in line with a narrowing of this angle due to the substitution with the Fxyl substituents compared to the pentafluoroethyl group.

However, the Cl–Sb–S angle is the most obtuse with 171.4(1)°. The Sb–S/Cl bonds are even longer than in **6**, **7** and **8**. Only the P–S bond is shorter than in the pentafluoroethyl-substituted analogue (Table 1).

The NMR data show a high field shift for the P–H unit in proton NMR for O → S and (F_5C_2) → (Fxyl), respectively. For the ^{31}P resonances a low-field shift in the same order is observed.

Starting from **3** and nBu$_3$SnH, we have succeeded in synthesising and isolating hydridostibane HSb(C_2F_5)$_2$ (**10**, Scheme 3). In addition to the analogous pentafluoroethyl-substituted nitrogen,[33] phosphorus[34] and bismuth[35] analogues, **10** is a highly reactive volatile compound that fumes strongly on contact with traces of moisture or oxygen and decomposes slowly at temperatures above −30 °C. However, an *in situ*-grown single crystal of **10** allowed for the determination of its solid-state structure (Fig. 7). In comparison with **3**, the Sb–C bond lengths in **10** are slightly shorter. Due to the significantly lower steric demand of the hydrogen atom instead of the chlorine atom, the C–Sb–C angle in **10** is about 9° larger.

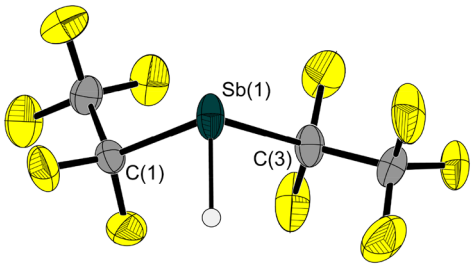

Fig. 7 Molecular structure of the hydridostibane HSb(C_2F_5)$_2$ (**10**) in the solid state. Ellipsoids are set at 50% probability. The disorder of one pentafluoroethyl group is not shown. Selected bond lengths [Å] and angles [°]: Sb(1)–C(1) 2.219(1), Sb(1)–C(3) 2.214(1); C(1)–Sb(1)–C(3) 94.4(1).

As with the other homologues with this substitution pattern, the proton resonance at 7.28 ppm in C_6D_6 (8.11 ppm in CD_2Cl_2) shows a complex splitting pattern. This is caused by coupling to the magnetically non-equivalent fluorine atoms of the CF_2 unit and to the trifluoromethyl groups. Fig. 8 shows that the experimental (top) and the simulated (bottom) multiplet patterns are in good agreement.[36] The underlying fitted coupling constants for the AA′BB′H spin system in **10** and their assignment are also given.

In the IR spectrum of gaseous **10**, we detected a band at 1919 cm^{-1} for the Sb–H vibration, which is within the typical range for this type of stretching frequency.[37]

The Gutmann–Beckett test allows an assessment to be made about the Lewis acidity of the compounds. The so-called acceptor number (AN) is calculated based on the ^{31}P NMR shift of the adduct of the Lewis acid with OP(Et)$_3$.[38] With AN values of 52.3 (**3**), 52.5 (**5**) and 29.8 (**10**), the stibanes **3** and **5** are in the upper mid-range of Gutmann's original scale from 0 (for hexane) to 100 (for $SbCl_5$); according to the test, **10** is significantly less Lewis acidic than **3** and **5**.

We tried to react hydridostibane **10** with the phosphane oxide H(O)P(tBu)$_2$ and the phosphane sulphide H(S)P(tBu)$_2$, expecting the formation of the adducts (C_2F_5)$_2$Sb(H)–O–P(H)(tBu)$_2$ and (C_2F_5)$_2$Sb(H)–S–P(H)(tBu)$_2$, which would be the formally hydrogen-loaded FLPs. In the samples of these reactions we

Table 2 Chemical shifts of the P–**H** unit in proton and ^{31}P{^{1}H} NMR spectra with the $^1J_{P,H}$ coupling constant (from ^{1}H NMR) of the phosphane oxide and sulphide reactants and the compounds **6** and **7**, (F_5C_2)$_2$(Cl)Sb(E)P(H)(tBu)$_2$, and **8** and **9**, (Fxyl)$_2$(Cl)Sb(E)P(H)(tBu)$_2$, with E = O or S in CD_2Cl_2

	^{1}H P–**H** [ppm]	$^1J_{P,H}$ [Hz]	^{31}P{^{1}H} P–**H** [ppm]
H(O)P(tBu)$_2$	6.01	424	64.7
H(S)P(tBu)$_2$	5.82	418	75.0
6 (E = O)	6.03	447	71.6
7 (E = S)	5.77	420	72.3
8 (E = O)	5.85	436	70.2
9 (E = S)	5.69	420	74.2

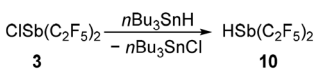

Scheme 3 Synthesis of **10** from **3** and nBu$_3$SnH.

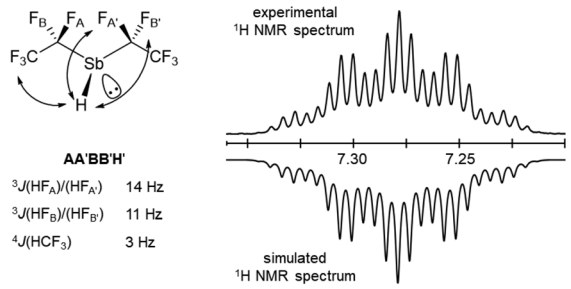

Fig. 8 Optimised coupling constants of **10** (left) and highlighted area of the experimental and simulated Sb–**H** region of the ^{1}H NMR spectrum of **10** in C_6D_6 (right).[34]

detected all the NMR signals of the reactants, but only the reaction of the sample containing the phosphane oxide showed a slight deviation in the NMR shifts relative to the reactants. For the mixture of **10** with phosphane sulphide there is no evidence of an interaction or reaction. However, attempts to isolate the product of the conversion of **10** with $H(O)P(tBu)_2$ failed and undefinable decomposition products were observed.

The mixture of **10** with $H(O)P(tBu)_2$ was also investigated by diffusion NMR experiments. The hydrodynamic volumes of **10** and the phosphane oxide in the mixture were found to be only slightly larger compared to those of the pure reactants. This does not allow for any clear conclusions to be drawn about the reaction of the two reactants.

$Fxyl_2SbH$ could not be synthesised from **7** and nBu_3SnH by a procedure analogous to that for **10**, so it was not possible to investigate any adducts that might be formed.

Conclusions

The presented $R^F{}_2Sb(Cl)–E–(H)P(tBu)_2$ (R^F = C_2F_5, 3,5-$(CF_3)_2C_6H_3$; E = O, S) systems, based on the corresponding chlorostibanes and phosphane chalcogenides, were found to be stable against HCl elimination. Even attempts to abstract hydrogen chloride under more severe reaction conditions failed. The angle of the bridging Sb–E–P unit in the adducts is significantly narrower for compounds with the higher homologue sulphur than for oxygen. The pentafluoroethyl groups cause a widening of this angle, as can be seen from the comparison with the Fxyl groups on the antimony atom in the corresponding solid-state structures. The hydridostibane $HSb(C_2F_5)_2$, obtained from the reaction of $ClSb(C_2F_5)_2$ with nBu_3SnH, seems to interact weakly with di-*tert*-butylphosphane oxide as revealed by slight shifts of the resonances in the NMR spectra. For a mixture of $HSb(C_2F_5)_2$ with di-*tert*-butylphosphane sulphide, comparable behaviour was not observed.

Author contributions

J. Krieft: investigation, methodology, validation, visualization, and writing (original draft); H. Koch: investigation (supporting synthesis); J.-H. Lamm: investigation (SCXRD); B. Neumann: investigation (SCXRD); H.-G. Stammler: investigation (SCXRD); A. Mix: investigation (diffusion NMR); and N. W. Mitzel: funding acquisition, project administration, supervision, reviewing and editing.

Data availability

The data published in this contribution are available as the ESI,† submitted with the manuscript. Crystallographic data have been deposited with the Cambridge Crystal Structure Database (CCDC).

Conflicts of interest

There are no conflicts to declare.

Acknowledgements

The authors thank Marco Wißbrock for recording NMR spectra and Barbara Teichner for performing elemental analyses. This work was supported by Deutsche Forschungsgemeinschaft (grant MI477/44-1, project number 461833739).

Notes and references

1 H. C. Brown, H. I. Schlesinger and S. Z. Cardon, *J. Am. Chem. Soc.*, 1942, **64**, 325–329.
2 (*a*) G. C. Welch, R. R. San Juan, J. D. Masuda and D. W. Stephan, *Science*, 2006, **314**, 1124–1126; (*b*) G. C. Welch and D. W. Stephan, *J. Am. Chem. Soc.*, 2007, **129**, 1880–1881; (*c*) D. W. Stephan, *J. Am. Chem. Soc.*, 2015, **137**, 10018–10032; (*d*) D. W. Stephan and G. Erker, *Chem. Sci.*, 2014, **5**, 2625–2641; (*e*) S. Döring, G. Erker, R. Fröhlich, O. Meyer and K. Bergander, *Organometallics*, 1998, **17**, 2183–2187.
3 T. Thorwart, D. Hartmann and L. Greb, *Chem. – Eur. J.*, 2022, **28**, e202202273.
4 B. Waerder, M. Pieper, L. A. Körte, T. A. Kinder, A. Mix, B. Neumann, H.-G. Stammler and N. W. Mitzel, *Angew. Chem., Int. Ed.*, 2015, **54**, 13416–13419.
5 T. A. Kinder, R. Pior, S. Blomeyer, B. Neumann, H.-G. Stammler and N. W. Mitzel, *Chem. – Eur. J.*, 2019, **25**, 5899–5903.
6 P. Holtkamp, F. Friedrich, E. Stratmann, A. Mix, B. Neumann, H.-G. Stammler and N. W. Mitzel, *Angew. Chem., Int. Ed.*, 2019, **58**, 5114–5118.
7 (*a*) M. Pieper, J.-H. Lamm, B. Neumann, H.-G. Stammler and N. W. Mitzel, *Dalton Trans.*, 2017, **46**, 5326–5336; (*b*) D. Salusso, G. Grillo, M. Manzoli, M. Signorile, S. Zafeiratos, M. Barreau, A. Damin, V. Crocellà, G. Cravotto and S. Bordiga, *ACS Appl. Mater. Interfaces*, 2023, **15**, 15396–15408.
8 (*a*) R. C. Neu, E. Otten, A. Lough and D. W. Stephan, *Chem. Sci.*, 2011, **2**, 170–176; (*b*) A. M. Chapman, M. F. Haddow and D. F. Wass, *J. Am. Chem. Soc.*, 2011, **133**, 8826–8829; (*c*) Z. Chen, Y. Ye, X. Feng, Y. Wang, X. Han, Y. Zhu, S. Wu, S. Wang, W. Yang, L. Wang and J. Zhang, *Nat. Commun.*, 2023, **14**, 2000; (*d*) K. Chang, X. Wang, Z. Fan and X. Xu, *Inorg. Chem.*, 2018, **57**, 8568–8580; (*e*) P. Jochmann and D. W. Stephan, *Angew. Chem., Int. Ed.*, 2013, **52**, 9831–9835.
9 (*a*) C. Appelt, H. Westenberg, F. Bertini, A. W. Ehlers, J. C. Slootweg, K. Lammertsma and W. Uhl, *Angew. Chem., Int. Ed.*, 2011, **50**, 3925–3928; (*b*) L. Keweloh, H. Klöcker, E.-U. Würthwein and W. Uhl, *Angew. Chem., Int. Ed.*, 2016, **55**, 3212–3215; (*c*) P. Federmann, R. Müller, F. Beckmann,

C. Lau, B. Cula, M. Kaupp and C. Limberg, *Chem. – Eur. J.*, 2022, **28**, e202200404; (*d*) A. F. G. Maier, S. Tussing, T. Schneider, U. Flörke, Z.-W. Qu, S. Grimme and J. Paradies, *Angew. Chem., Int. Ed.*, 2016, **55**, 12219–12223; (*e*) K. Samigullin, I. Georg, M. Bolte, H.-W. Lerner and M. Wagner, *Chem. – Eur. J.*, 2016, **22**, 3478–3484; (*f*) H. Li, A. J. A. Aquino, D. B. Cordes, F. Hung-Low, W. L. Hase and C. Krempner, *J. Am. Chem. Soc.*, 2013, **135**, 16066–16069.

10 (*a*) D. W. Stephan and G. Erker, *Angew. Chem., Int. Ed.*, 2010, **49**, 46–76; (*b*) C. M. Mömming, E. Otten, G. Kehr, R. Fröhlich, S. Grimme, D. W. Stephan and G. Erker, *Angew. Chem., Int. Ed.*, 2009, **48**, 6643–6646; (*c*) D. W. Stephan, *Dalton Trans.*, 2009, 3129–3136; (*d*) A. E. Ashley, A. L. Thompson and D. O'Hare, *Angew. Chem., Int. Ed.*, 2009, **48**, 9839–9843; (*e*) C. Manankandayalage, D. K. Unruh and C. Krempner, *Chem. – Eur. J.*, 2021, **27**, 6263–6273; (*f*) O. J. Metters, S. J. K. Forrest, H. A. Sparkes, I. Manners and D. F. Wass, *J. Am. Chem. Soc.*, 2016, **138**, 1994–2003.

11 D. W. Stephan and G. Erker, *Angew. Chem., Int. Ed.*, 2015, **54**, 6400–6441.

12 P. Holtkamp, D. Poier, B. Neumann, H.-G. Stammler and N. W. Mitzel, *Chem. – Eur. J.*, 2021, **27**, 3793–3798.

13 J. Krieft, P. C. Trapp, Y. V. Vishnevskiy, B. Neumann, H.-G. Stammler, J.-H. Lamm and N. W. Mitzel, *Chem. Sci.*, 2024, **15**, 12118–12125.

14 J. Krieft, B. Neumann, H.-G. Stammler and N. W. Mitzel, *Dalton Trans.*, 2024, **53**, 11762–11768.

15 R. G. Pearson, *J. Am. Chem. Soc.*, 1963, **85**, 3533–3539.

16 (*a*) B. Pan and F. P. Gabbaï, *J. Am. Chem. Soc.*, 2014, **136**, 9564–9567; (*b*) D. Tofan and F. P. Gabbaï, *Chem. Sci.*, 2016, **7**, 6768–6778; (*c*) C.-H. Chen and F. P. Gabbaï, *Angew. Chem., Int. Ed.*, 2017, **56**, 1799–1804; (*d*) C.-H. Chen and F. P. Gabbaï, *Dalton Trans.*, 2018, **47**, 12075–12078; (*e*) G. Park, D. J. Brock, J.-P. Pellois and F. P. Gabbaï, *Chem*, 2019, **5**, 2215–2227; (*f*) M. Yang, M. Hirai and F. P. Gabbaï, *Dalton Trans.*, 2019, **48**, 6685–6689; (*g*) G. Park and F. P. Gabbaï, *Chem. Sci.*, 2020, **11**, 10107–10112; (*h*) D. You, B. Zhou, M. Hirai and F. P. Gabbaï, *Org. Biomol. Chem.*, 2021, **19**, 4949–4957; (*i*) V. M. Gonzalez, G. Park, M. Yang and F. P. Gabbaï, *Dalton Trans.*, 2021, **50**, 17897–17900; (*j*) B. L. Murphy and F. P. Gabbaï, *J. Am. Chem. Soc.*, 2023, **145**, 19458–19477.

17 J. L. Beckmann, J. Krieft, Y. V. Vishnevskiy, B. Neumann, H.-G. Stammler and N. W. Mitzel, *Angew. Chem., Int. Ed.*, 2023, **62**, e202310439.

18 J. L. Beckmann, J. Krieft, Y. V. Vishnevskiy, B. Neumann, H.-G. Stammler and N. W. Mitzel, *Chem. Sci.*, 2023, **14**, 13551–13559.

19 D. Zhu, Z.-W. Qu and D. W. Stephan, *Dalton Trans.*, 2020, **49**, 901–910.

20 Y. Wang, Z. H. Li and H. Wang, *RSC Adv.*, 2018, **8**, 26271–26276.

21 L. Wickemeyer, N. Aders, A. Mix, B. Neumann, H.-G. Stammler, J. J. Cabrera-Trujillo, I. Fernández and N. W. Mitzel, *Chem. Sci.*, 2022, **13**, 8088–8094.

22 L. Wickemeyer, L. Hartmann, B. Neumann, H.-G. Stammler and N. W. Mitzel, *Chem. – Eur. J.*, 2022, e202202842.

23 M. Ates, H. J. Breunig, A. Soltani-Neshan and M. Tegeler, *Z. Naturforsch.*, 1986, **41B**, 321–326.

24 D. Naumann, G. Nowicki and K.-J. Sassen, *Z. Anorg. Allg. Chem.*, 1997, **623**, 1183–1189.

25 F. Dornhaus, H.-W. Lerner and M. Bolte, *Acta Crystallogr., Sect. E: Struct. Rep. Online*, 2005, **61**, o657–o658.

26 G. Y. Li and W. J. Marshall, *Organometallics*, 2002, **21**, 590–591.

27 A. Haaland, V. I. Sokolov, H. V. Volden, H. J. Breunig, M. Denker and R. Rösler, *Z. Naturforsch.*, 1997, **52B**, 296–300.

28 A. Haaland, D. J. Shorokhov, V. I. Sokolov, H. V. Volden, H. J. Breunig, M. Denker and R. Rösler, *Phosphorus, Sulfur Silicon Relat. Elem.*, 1998, **136**, 463–466.

29 A. Almenningen, O. Bastiansen, V. Ewing, K. Hedberg and M. Traetteberg, *Acta Chem. Scand.*, 1963, **17**, 2455–2460.

30 A. Almenningen, K. Hedberg and R. Seip, *Acta Chem. Scand.*, 1963, **17**, 2264–2270.

31 W. Airey, C. Glidewell, A. G. Robiette and G. M. Sheldrick, *J. Mol. Struct.*, 1971, **8**, 413–422.

32 W. Airey, C. Glidewell, D. W. H. Rankin, A. G. Robiette, G. M. Sheldrick and D. W. J. Cruickshank, *Trans. Faraday Soc.*, 1970, **66**, 551.

33 K. E. Peterman and J. M. Shreeve, *Inorg. Chem.*, 1975, **14**, 1223–1228.

34 A. V. Zakharov, Y. V. Vishnevskiy, N. Allefeld, J. Bader, B. Kurscheid, S. Steinhauer, B. Hoge, B. Neumann, H.-G. Stammler, R. J. F. Berger and N. W. Mitzel, *Eur. J. Inorg. Chem.*, 2013, 3392–3404.

35 S. Solyntjes, J. Bader, B. Neumann, H.-G. Stammler, N. Ignat'ev and B. Hoge, *Chem. – Eur. J.*, 2017, **23**, 1557–1567.

36 P. H. Budzelaar, *gNMR Version 5.0*, IvorySoft, 2006.

37 D. W. H. Rankin, C. A. Morrison and N. W. Mitzel, *Structural Methods in Molecular Inorganic Chemistry*, John Wiley & Sons, Inc., Chichester, West Sussex, U.K., 1st edn, 2013.

38 (*a*) M. A. Beckett, G. C. Strickland, J. R. Holland and K. S. Varma, *Polymer*, 1996, **37**, 4629–4631; (*b*) U. Mayer, V. Gutmann and W. Gerger, *Monatsh. Chem.*, 1975, **106**, 1235–1257.

